J. Phys.: Condens. Matter **11** (1999) 6337–6346. Printed in the UK PII: S0953-8984(99)03943-0

Crystal structure and cation distributions in the $FeTi_2O_5$–Fe_2TiO_5 solid solution series

W Q Guo†‡, S Malus†, D H Ryan† and Z Altounian†

† Centre for the Physics of Materials, Department of Physics, McGill University, Montreal, Quebec, Canada H3A 2T8

‡ State Key Laboratory of RSA, Institute of Metal Research, Chinese Academy of Sciences, 72 Wenhua Road, Shenyang 110015, People's Republic of China

E-mail: dominic@physics.mcgill.ca (D H Ryan)

Received 5 May 1999

Abstract. The $Fe_{1+x}Ti_{2-x}O_5$, $0 \leqslant x \leqslant 1$, solid solution series has been systematically investigated by means of x-ray diffraction, Mössbauer spectroscopy and neutron diffraction. The results confirm that the $Fe_{1+x}Ti_{2-x}O_5$, $0 \leqslant x \leqslant 1$ pseudobrookite series has an orthorhombic structure with the D_{2h}^{17} ($Cmcm$) space group. The unit cell contains four formula units. The site occupancies obtained from both Mössbauer spectra and neutron diffraction data indicate that the cation (Fe^{2+}, Fe^{3+} and Ti^{4+}) distributions in the available sites, 4c and 8f, are neither random nor perfectly ordered. At $x = 0$, most of the iron is in the 4c site, and the 8f site fills progressively as $x \to 1$. The agreement between the Mössbauer and neutron site occupancies indicates that the Fe^{3+} and Fe^{2+} site preferences are the same.

1. Introduction

Titanium-substituted iron oxides are widespread in nature and represent an important mineral resource for the commercial extraction of both iron and titanium. The Fe–Ti–O phase diagram contains a variety of solid-solution minerals [1] including ulvospinel–magnetite ($Fe_{3-x}Ti_xO_4$), ilmenite–haematite ($Fe_{2-x}Ti_xO_3$) and pseudobrookite ($Fe_{1+x}Ti_{2-x}O_5$), the subject of this work. This tie-line in the Fe–Ti–O phase diagram links ferric pseudobrookite ($x = 1$) with ferrous pseudobrookite ($x = 0$); however the latter is only stable above 1135 °C [2]. While it is not a commonly occurring mineral, pseudobrookite is of both commercial and scientific interest. It is produced in substantial quantities during the processing of ilmenite ores as a by-product of iron and titanium extraction [3]. Pseudobrookite more recently acquired a non-terrestrial significance as an oxygen source for lunar bases for which an oxidation–reduction cycle on high-ilmenite soils and volcanic glasses has been demonstrated to work [4, 5]. Finally, at low temperatures, ferric pseudobrookite (Fe_2TiO_5) exhibits an anisotropic spin glass phase [6] that has drawn a lot of attention [7–9].

Understanding the magnetic properties of the pseudobrookite series demands a complete description of the crystal and chemical structures of the compounds. Pauling [10] first reported that pseudobrookite had an orthorhombic crystal structure in 1930. However, little further progress was made until Akimoto *et al* successfully synthesized the solid solution series, $Fe_{1+x}Ti_{2-x}O_5$, $0 \leqslant x \leqslant 1$ in 1957 [11]. Wyckoff [12] summarized the crystal structure of ferric pseudobrookite, Fe_2TiO_5, as orthorhombic, containing four formula units per unit cell and belonging to the space group D_{2h}^{17} ($Cmcm$). Despite the lack of contrast between Fe and

0953-8984/99/336337+10$30.00

Ti in x-ray diffraction data, it was assumed that the metal ions were perfectly ordered, i.e. that Fe and Ti atoms occupied the 8f and 4c sites, respectively. This assignment was retained by Hamelin [13]. Lind and Housley [14] argued that Hamelin's data are more compatible with iron in both sites: four Fe^{3+} filling the 4c and four Fe^{3+} and four Ti^{4+} in 8f. Shirane *et al* [15] studied the Mössbauer spectra of both ferrous ($x = 0$) and ferric ($x = 1$) pseudobrookite. They preferred Wyckoff's assignment of all Fe^{3+} being in the 8f site for $x = 1$, and argued that for $x = 0$, a distribution in which the 4c remained filled by Ti, and the 8f was occupied by 4 Fe^{2+} and 4 Ti, was more plausible. However, the observed asymmetry in their spectrum indicated the presence of two distinct iron types. Muranaka *et al* [16] measured ^{57}Fe Mössbauer spectra of Fe_2TiO_5 and $FeTi_2O_5$ at temperatures between 4 K and 300 K. They basically retained the assignment of Shirane *et al* [15] for $FeTi_2O_5$ and that of Wyckoff [12] for Fe_2TiO_5 although they noted that the form of the spectrum at 4 K clearly indicated that some of the Fe^{3+} ions were located in the 4c sites of Fe_2TiO_5. Atzmony *et al* [6] and Gurewitz and Atzmony [17] reported that the isomer shift and quadrupole splitting for Fe_2TiO_5 were typical of high spin Fe^{3+} for $T > 55$ K. Furthermore, they argued that the intensity of the (112) peak in the neutron diffraction pattern at 295 K for Fe_2TiO_5 indicated that the Fe^{3+} and Ti^{4+} ions were essentially randomly distributed between the 8f and 4c sites. However, they only report a single Fe^{3+} site in the 300 K Mössbauer spectrum. By contrast, Cruz *et al* [18] report two Fe^{3+} sites but invoke a substantial (more than a factor of two) difference in recoil-free fractions between the two sites in order to match the apparent areas of the two contributions with an assumed random distribution of iron ions between the 4c and 8f sites. Grey and Ward [19] recorded the Mössbauer spectrum of $FeTi_2O_5$, and assigned 28% of the Fe^{2+} to the 8f sites and 72% to the 4c sites, a distribution which corresponds closely to the site occupancy (75%) that they had determined from neutron diffraction measurements for this compound. Finally, there are also two claims that Fe_2TiO_5 occurs in a monoclinic structure with different space groups ($C2/c$ [20] or $C2$ [21]) and unrelated lattice parameters.

Given the wide disparity in structures and site occupations reported for this system, we have carried out a systematic study of the $Fe_{1+x}Ti_{2-x}O_5$, $0 \leqslant x \leqslant 1$, solid solution series using Mössbauer spectroscopy and neutron diffraction. The samples are orthorhombic at all compositions and we obtained complete agreement between site occupancies derived from Mössbauer and neutron measurements.

2. Experimental methods

Samples were synthesized by mixing the starting powder materials, Fe (99.9% purity), Fe_2O_3 (99.8%) and TiO_2 (99.9%), in stoichiometric amounts, according to the following reaction:

$$\frac{(1+2x)}{3}Fe_2O_3 + (2-x)TiO_2 + \frac{(1-x)}{3}Fe \longrightarrow Fe_{1+x}Ti_{2-x}O_5 \qquad (1)$$

to provide Fe:Ti:O ratios of $(1+x):(2-x):5(0.0 \leqslant x \leqslant 1.0)$, following the method of Akimoto *et al* [11]. Prior to weighing, the starting materials were dried in air for at least 24 hours at 200 °C. The mixture was homogenized by co-grinding in an agate mortar and formed into a pellet using a hydraulic press. The pelletizing procedure was employed to reduce the possibility of Fe reacting with the quartz tube at high temperatures since only point contacts were made between the pellets and the tube. The pellets were further dried at 200 °C in air, then sintered for two hours at 1170–1300 °C in sealed quartz tubes containing 200 mbar of He. One of the end numbers, Fe_2TiO_5, was also annealed in air with various ratios of Fe_2O_3:TiO_2 from 50:50 to 47:53 to reduce the remained haematite in Fe_2TiO_5. After quenching to room temperature, the pellets were powdered and checked by x-ray powder diffraction on a Nicolet-Stöe automated

powder diffractometer using graphite monochromated Cu Kα radiation. Mössbauer spectra were obtained at room temperature on a conventional constant-acceleration spectrometer with a 0.2 GBq ^{57}Co**Rh** source. The spectra were fitted using a standard non-linear least-squares minimization routine employing a sum of Lorentzian lines. The spectrometer was calibrated against an α-Fe foil at room temperature.

Neutron diffraction patterns were collected on the C-2 800-wire Dualspec powder diffractometer at Chalk River Laboratories, Ontario. The wavelength of 1.2357 Å was determined using a 99.9999% Si powder standard. A total of 34 parameters were refined using GSAS [22] in order to fit the diffraction patterns. These were: lattice parameters, locations and thermal factors for each of the 4c and 8f metal sites, fraction of 4c occupied by Fe, fraction of 8f occupied by Fe (the metal sites were constrained to be fully occupied, so the balance in each site was Ti), locations and (linked) thermal factors for the three oxygen sites, with angle-dependent background and resolution functions.

3. Results and discussion

Twelve $Fe_{1+x}Ti_{2-x}O_5$ ($x = 0.0, 0.05, 0.1, 0.2, \ldots, 1.0$) samples were synthesized under various experimental conditions. X-ray diffraction patterns for the 12 samples show that 11 samples were single phase; an extra diffraction peak occurred at $2\theta \approx 27.7^\circ$ in the x-ray pattern for $FeTi_2O_5$ indicating that a small amount of a second phase is present. However it was impossible to determine the structure of this impurity phase from a single diffraction peak.

We emphasize that no diffraction peaks occurred at $2\theta < 10^\circ$ in any of the samples prepared for this study. We therefore found no evidence for the monoclinic phase reported by Shiojiri *et al* [21].

Typical ^{57}Fe Mössbauer spectra for the $Fe_{1+x}Ti_{2-x}O_5$, $0 \leqslant x \leqslant 1$, samples at room temperature are shown in figure 1. As can be observed, the spectrum for Fe_2TiO_5 shows a broad doublet corresponding to Fe^{3+}, while the spectrum for $FeTi_2O_5$ consists of a strong sharp doublet together with a weaker broad doublet (shoulders on the inner side of each line) with a smaller quadrupole splitting. It appears to be difficult to obtain clean single phase samples of the end members, Fe_2TiO_5 and $FeTi_2O_5$, as several authors [15, 16, 18] have mentioned the existence of impurity phases in their samples. Mössbauer spectroscopy revealed traces

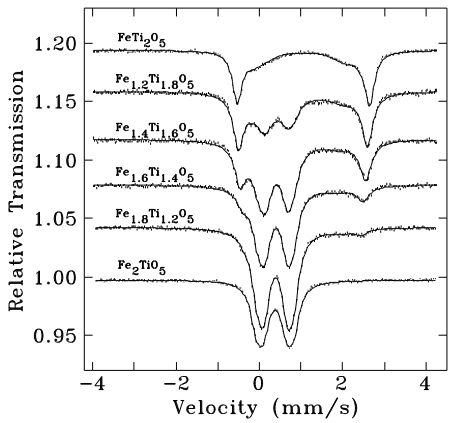

Figure 1. Mössbauer spectra for the $Fe_{1+x}Ti_{2-x}O_5$ solid solution series at room temperature. Fits are shown as solid lines.

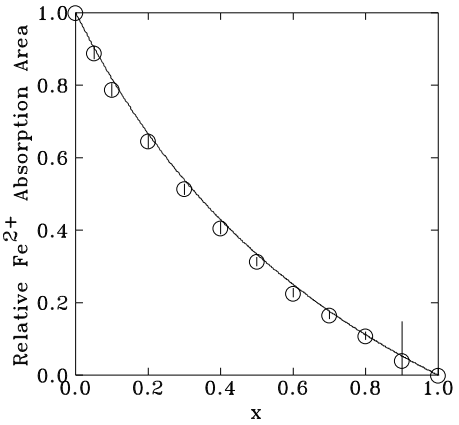

Figure 2. Fe^{2+} fraction in $Fe_{1+x}Ti_{2-x}O_5$. The solid line was calculated using equation (2).

of ulvospinel or ilmenite remaining in all of the $FeTi_2O_5$ samples and a trace of haematite in some of the Fe_2TiO_5 samples. These secondary phases were not detected by x-ray diffraction, suggesting that it is difficult to identify whether a sample is single phase or not by only x-ray diffraction, especially in cases where the diffraction lines overlap strongly and no extra diffraction peaks can be seen. In some cases we detected significant amounts of haematite by neutron diffraction in samples that showed no contamination by x-ray diffraction. We attribute these differences to the superior penetrating power of neutrons and Mössbauer gamma-rays which provide better bulk probes than x-rays. We obtained a very clean ferric pseudobrookite sample, after adding extra TiO_2 into the starting mixture of TiO_2 and Fe_2O_3 in order to reduce the haematite content in Fe_2TiO_5 as detected with Mössbauer spectroscopy.

Examination of figure 1 reveals that all of the iron ions in $FeTi_2O_5$ appear to be Fe^{2+}, and those in Fe_2TiO_5 are Fe^{3+}, while both Fe^{2+} and Fe^{3+} coexist in $Fe_{1+x}Ti_{2-x}O_5$. Indeed, the spectra for $x \neq 0, 1$ can almost be fitted as a linear combination of the $x = 1$ and $x = 0$ spectra. Since the two valence states of the iron can be so readily distinguished, the relative Mössbauer absorption areas of the Fe^{3+} and Fe^{2+} components can be used as an indicator of chemical composition. According to the following chemical reaction:

$$Fe_{1+x}Ti_{2-x}O_5 = (1-x)FeTi_2O_5 + xFe_2TiO_5 \tag{2}$$

the ratio between Fe^{2+} and the total iron content (Fe_{tot}) in the system can be expressed as:

$$\frac{Fe^{2+}}{Fe_{tot}} = \frac{1-x}{1+x}. \tag{3}$$

Figure 2 shows the relative Mössbauer absorption area for Fe^{2+} together with the prediction of equation (3) and the excellent agreement confirms that the samples have the correct stoichiometric ratio between Fe^{3+} and Fe^{2+}. The amount of Fe^{2+} decreases with increasing x demonstrating that the chemical reaction process to form this solid solution series is described correctly by equation (2).

Inspection of figure 1, and the fitted Mössbauer parameters listed in table 1, confirm that there are two sites for each of the Fe^{3+} and Fe^{2+} components, that they have distinct quadrupole splittings (Δ) and isomer shifts (δ), and that these parameters evolve smoothly across the series. These results are fully consistent with the availability of two sites in the orthorhombic crystal structure, and incompatible with one site in the monoclinic structure suggested by Shiojiri *et al* [21]. Furthermore, it is clear that Fe occurs in both the 8f and 4c sites at all compositions

Table 1. The fitted parameters derived from the Mössbauer spectra for the Fe^{2+} and Fe^{3+} components. Isomer shift (δ) and quadrupole splitting (Δ).

	$FeTi_2O_5$ (Fe^{2+})				
	8f		4c		
x	δ	Δ	δ	Δ	Fe^{2+} area
0.0	1.10 ± 0.01	2.16 ± 0.03	1.064 ± 0.001	3.148 ± 0.003	100.0
0.2	1.10 ± 0.03	1.91 ± 0.09	1.047 ± 0.002	3.094 ± 0.004	64.52
0.4	1.12 ± 0.04	1.97 ± 0.12	1.043 ± 0.003	3.023 ± 0.006	40.53
0.6	1.05 ± 0.04	1.69 ± 0.14	1.051 ± 0.005	2.877 ± 0.012	22.68
0.8	1.20 ± 0.03	1.56 ± 0.10	1.042 ± 0.012	2.807 ± 0.031	19.94
	Fe_2TiO_5 (Fe^{3+})				
	8f		4c		
x	δ	Δ	δ	Δ	Fe^{3+} area
0.2	0.409 ± 0.007	0.58 ± 0.02	0.337 ± 0.019	1.05 ± 0.04	35.48
0.4	0.411 ± 0.005	0.54 ± 0.02	0.376 ± 0.010	0.87 ± 0.06	59.47
0.6	0.401 ± 0.002	0.54 ± 0.02	0.391 ± 0.002	0.85 ± 0.02	77.32
0.8	0.395 ± 0.001	0.55 ± 0.01	0.389 ± 0.002	0.88 ± 0.01	89.06
1.0	0.382 ± 0.001	0.57 ± 0.01	0.379 ± 0.002	0.92 ± 0.01	100.0

of pseudobrookite. This observation immediately allows us to rule out fully ordered metal distributions.

The site occupancies of Fe^{2+} in this solid solution series based on Mössbauer analysis are shown in figure 3. According to Wyckoff [12] and the neutron structure refinement below, the two metal sites in Fe_2TiO_5 are octahedrally coordinated with different distortions. The 4c sites are surrounded by a fairly regular octahedron of oxygen ions at distances between 1.90 Å and 1.99 Å, while the 8f sites occupy a strongly distorted oxygen octahedron with four of the oxygen ions forming a tetrahedron at distances between 1.83 Å and 1.97 Å, with the remaining two situated at a distance of 2.31 Å. The isomer shifts and quadrupole splittings (listed in table 1) for $FeTi_2O_5$ are typical of high-spin Fe^{2+}. For this configuration, increasing distortion from a regular octahedron leads to a smaller quadrupole splitting [23]. Accordingly we assign the 68% of Fe^{2+} in $FeTi_2O_5$ to the 4c site because of their larger quadrupole splitting. Hence 68% of the 4c site is occupied by Fe^{2+} ions, and 16% of the 8f. This distribution is a long way from the 33% expected for a random distribution and will be confirmed by the neutron diffraction data below.

The Fe^{3+} site preferences in Fe_2TiO_5 obtained from Mössbauer analysis are 38(3)% and 62(5)%. Following the same reasoning as for Fe^{2+}, we assign the larger quadrupole splitting to the more regular site. This places 38% of Fe^{3+} in the 4c site and makes the site occupancy 77%. If we reverse the assignment and put the 38% into the 8f site, this requires that the remaining 62% of the Fe^{3+} occupies the 4c site and the filling of this site reaches an unreasonable 124%. Cruz *et al* [18] assumed that the recoil-free fractions of the two sites were vastly different in order to justify this latter site assignment. As we will show below, the agreement between the neutron and Mössbauer site occupations requires no such assumptions, and we conclude that 77% of the 4c site is occupied by Fe^{3+} and 62% of the 8f. While the Mössbauer occupations are each within error of the 67% expected from random occupation, the neutron diffraction results confirm the observed bias.

Neutrons provide a better probe of the crystal structure for several reasons. They are more penetrating so they are less affected by surface effects. The larger samples used can

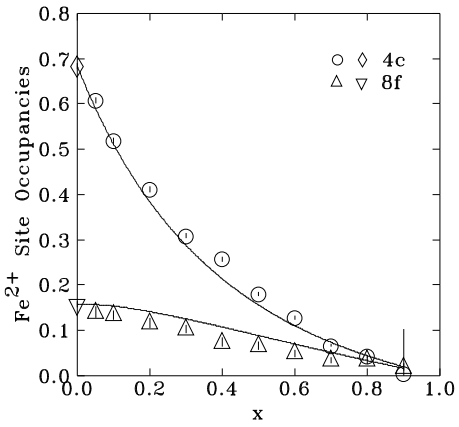

Figure 3. Fe^{2+} site occupancies derived from the fits to the Mössbauer spectra. Data for $FeTi_2O_5$ ($x = 0$) after correction for the presence of ulvospinel and ilmenite are shown as $\Diamond$ and $\triangledown$. The solid lines were obtained by combining the Fe^{2+} fraction expected from the stoichiometry with the site occupancies derived from refinement of the neutron diffraction patterns. They are not fits.

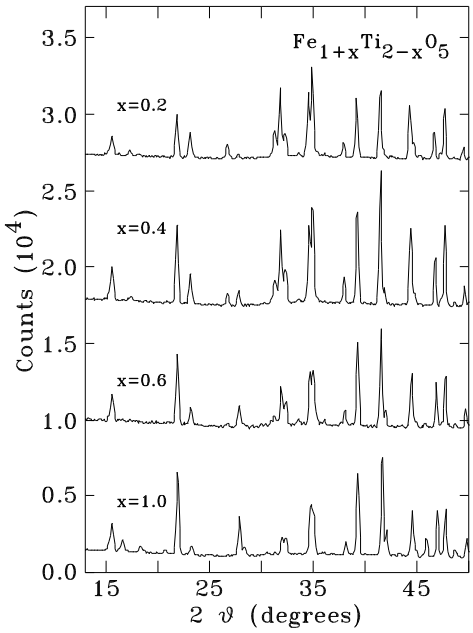

Figure 4. Typical neutron diffraction patterns for $Fe_{1+x}Ti_{2-x}O_5$. The changing distribution of Fe and Ti can be seen through the evolving intensities of the reflections at 23° and 24°, and the doublet at 35°.

be more readily randomized (they were also rotated during the measurement) so that texture effects can be minimized making a more detailed analysis of line intensities possible. The scattering lengths of Fe and Ti are both large and of opposite sign ($b_{Ti} = -3.44 \times 10^{-26}$ m^2, $b_{Fe} = +9.45 \times 10^{-26}$ m^2) making the contrast between these two species extremely large. Typical neutron diffraction patterns at room temperature are shown in figure 4 for the series,

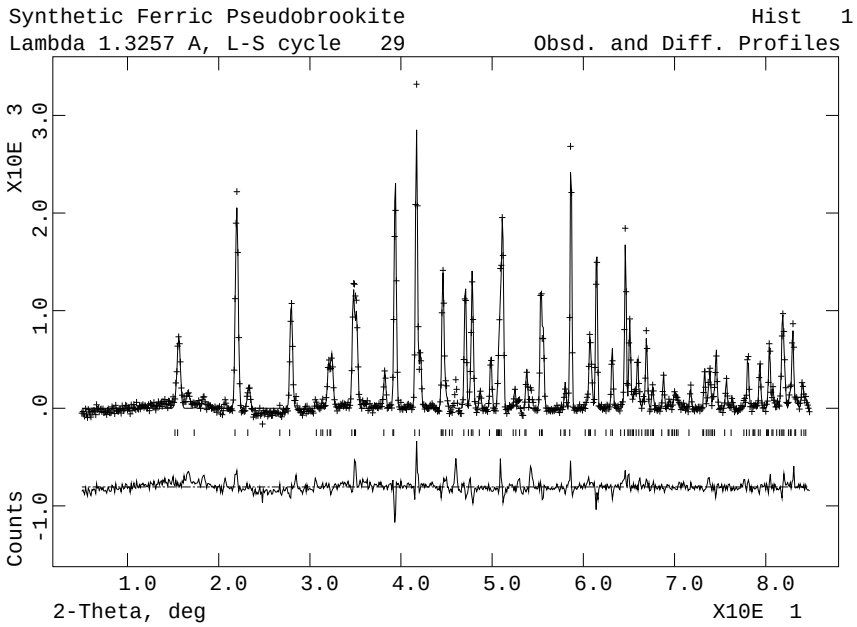

Figure 5. Neutron diffraction pattern for Fe_2TiO_5. Data are indicated by the +, and calculated pattern by the solid line. The difference pattern is shown at the bottom. The location of reflections is indicated by the small vertical bars.

while figure 5 shows the results of a GSAS fit for the $x = 1$ sample. The cell parameters and atomic locations derived from the fits are given in table 2. No extra low-angle reflections were observed, allowing us to rule out a monoclinic structure [20, 21] and the intensity refinements confirm the x-ray and Mössbauer conclusion of an orthorhombic cell. As the Fe^{3+} content increases, the unit cell parameters become smaller: a and c decrease slightly while b decreases more rapidly. Naturally, the unit cell parameters are associated with the effective ionic radii in the oxides, and as the Fe^{3+} content increases from $FeTi_2O_5$ to Fe_2TiO_5, the substitution process, $Fe^{2+} + Ti^{4+} \longrightarrow 2Fe^{3+}$, must occur simultaneously. The effective ionic radii of the cations [24] are 0.77 Å for Fe^{2+} high spin, 0.65 Å for Fe^{3+} low spin and 0.61 Å for Ti^{4+}. As a result of the substitution of Fe^{2+} and Ti^{4+} by $2Fe^{3+}$, the unit cell parameters gradually decrease from $FeTi_2O_5$ to Fe_2TiO_5. This continuous variation of cell parameters suggests that the basic pseudobrookite structure is retained throughout the solid solution series.

The extreme scattering contrast between Fe and Ti allows the chemical composition of the samples to be determined with great accuracy (typically better than $\pm 2\%$). This feature provides a robust check of our site and structure determination—if we have the incorrect cell parameters or space group, it is unlikely that we would be able to get the chemistry right. However, as is clear from figure 6, the analysis of the neutron diffraction data accurately yields the expected chemical composition in all cases.

Having established the correct crystal structure and chemical composition of the samples, we proceed to the final phase of the analysis: the determination of the site occupancies. The results in figure 7 show that the 4c site always contains more Fe than the 8f, and that the additional iron introduced as x increases from 0 to 1 is accommodated primarily in the 8f site. The compositional dependences of the two site occupancies are approximately linear in x and

Table 2. The unit cell parameters and atomic positions derived from analysis of the neutron diffraction patterns. Values shown in parentheses are estimated standard deviation in the least significant decimal place.

	Unit cell parameters			
x	a (Å)	b (Å)	c (Å)	Vol. (Å^3)
0.0	9.8081(7)	10.0710(8)	3.7503(3)	370.44
0.2	9.7936(3)	10.0430(3)	3.7466(1)	368.50
0.4	9.7859(3)	10.0219(3)	3.7445(1)	367.24
0.6	9.7834(4)	9.9982(4)	3.7394(2)	365.77
0.8	9.7914(4)	9.9898(4)	3.7377(2)	365.60
1.0	9.7933(5)	9.9786(5)	3.7318(2)	364.69

	Atomic positions					
	Fe_2TiO_5			$FeTi_2O_5$		
Sites	x	y	z	x	y	z
M_1(4c)	0.1884(8)	$\frac{1}{4}$	0	0.1922(10)	$\frac{1}{4}$	0
M_2(8f)	0.1367(7)	0.5649(7)	0	0.1315(22)	0.5619(23)	0
O_1(4c)	0.7617(8)	$\frac{1}{4}$	0	0.7805(8)	$\frac{1}{4}$	0
O_2(8f$_1$)	0.0480(6)	0.1167(5)	0	0.0458(6)	0.1134(6)	0
O_3(8f$_2$)	0.3108(6)	0.0709(5)	0	0.3138(7)	0.0633(6)	0

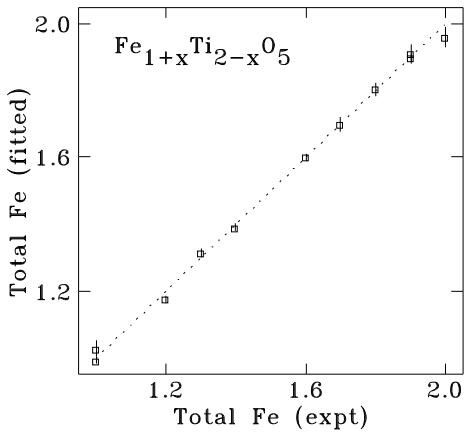

Figure 6. Comparison of iron contents derived from fitting the neutron diffraction patterns with those expected from the stoichiometry. The dotted line is simply a line of slope 1.

can be expressed as:

$$S_{4c} = 0.682(7) + 0.04(1)x \tag{4}$$

$$S_{8f} = 0.158(3) + 0.482(6)x \tag{5}$$

where S_{4c} and S_{8f} are the site occupancies in the 4c and 8f sites, respectively. It is clear from figure 7 that the Fe distribution is neither perfectly ordered nor particularly random. There is a clear bias towards Fe occupation of the 4c site that persists across the whole composition range, although the distribution does tend towards random with increasing x. Our site occupations are in closest agreement with the Mössbauer results of Grey and Ward [19].

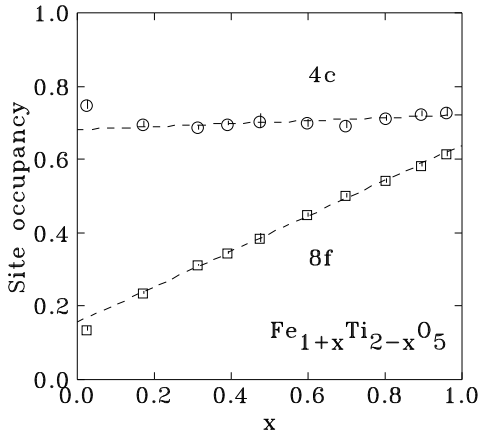

Figure 7. Fe site occupancies based on neutron diffraction data of $Fe_{1+x}Ti_{2-x}O_5$. The solid lines are linearly fitted results.

The site occupations presented in figure 7 confirm those assignments made earlier for the Mössbauer data. For example, the 72% occupancy of the 4c by Fe in Fe_2TiO_5 indicates that 36% of the total Fe is in this site, a result that is in perfect agreement with the $38 \pm 3\%$ obtained from the Mössbauer data for the same site. Moreover, we can combine equations (3), (4) and (5) to calculate the Fe^{2+} site occupancies in the 4c and 8f sites for comparison with the Mössbauer data. The results of this analysis are shown as solid lines in figure 3. We emphasize that these lines are not fits: they are derived from the confirmed stoichiometry (equation (3)) and the fitted neutron site occupancies (equations (4) and (5)) assuming that Fe^{2+} and Fe^{3+} exhibit identical site biases. The remarkable agreement between the neutron and Mössbauer results requires that the recoil-free fractions of the two sites are closely similar, as would be expected for iron atoms in similar environments, and in complete disagreement with the assumption of Cruz *et al* [18]. Furthermore, the site preferences of Fe^{2+} and Fe^{3+} must be the same.

4. Conclusion

We have systematically investigated the solid solution series, $Fe_{1+x}Ti_{2-x}O_5$, $0 \leqslant x \leqslant 1$, by means of x-ray diffraction, Mössbauer spectroscopy and neutron diffraction; the excellent agreement among the various results allows us to conclude the following.

(i) The $Fe_{1+x}Ti_{2-x}O_5$, $0 \leqslant x \leqslant 1$, solid solution series has an orthorhombic unit cell, containing four formula units per cell with space group D_{2h}^{17} ($Cmcm$). No evidence for a monoclinic structure was found under our experimental conditions.

(ii) Fe strongly prefers to occupy the 4c site, but moves into the 8f site as x increases. At no composition do we observe a random occupation of the two sites.

(iii) There is no significant difference between the Fe^{3+} and Fe^{2+} site preferences.

(iv) The agreement between the Mössbauer and neutron data on site occupations indicates that the recoil-free fractions for iron in the two sites are essentially the same.

Acknowledgments

This work was supported by the Natural Sciences and Engineering Research Council of Canada and le Fonds pour la Formation de Chercheurs et l'Aide à la Recherche de la Province du Québec. The authors would like to acknowledge the assistance provided by I Swainson of the neutron scattering group at Chalk River Laboratories.

References

[1] Taylor R W 1964 *Am. Mineral.* **49** 1016
[2] Eriksson G, Pelton A D, Woermann E and Ender A 1996 *Ber. Bunsenges. Phys. Chem.* **100** 1839
[3] Merk R and Pickles C A 1988 *Can. Metall. Q.* **3** 179
[4] Briggs R A and Sacco A Jr 1993 *Metall. Trans.* A **24** 1257
[5] Allen C A, Bond G G and McKay D S 1994 *Eng. Constr. Oper. in Space IV* (New York: Amer. Soc. Civil Eng.) p 1157
[6] Atzmony U, Gurewitz E, Melamud M, Pinto H, Shaked H, Gorodetsky G, Hermon E, Hornreich R M, Shtrikman S and Wanklyn B 1979 *Phys. Rev. Lett.* **43** 782
[7] Yeshurun Y, Felner I and Wanklyn B 1984 *Phys. Rev. Lett.* **53** 620
[8] Yeshurun Y and Sompolinsky H 1984 *Phys. Rev.* **31** 3191
[9] Brabers V A M, Boekema C, Lichti R L, Denison A B, Cooke D W, Heffner R H, Hutson R L, Schillaci M E and MacLaughlin D E 1987 *J. Appl. Phys.* **61** 4086
[10] Pauling L 1930 *Z. Kristallogr.* **73** 97
[11] Akimoto S, Nagata T and Katsura T 1957 *Nature* **179** 37
[12] Wyckoff R W G 1964 *Cryst. Struct.* **3** 297
[13] Hamelin M 1958 *Bull. Soc. Chim. France* **67** 1559
[14] Lind M D and Housley R M 1972 *Science* **175** 521
[15] Shirane G, Cox D E and Ruby S L 1962 *Phys. Rev.* **125** 1158
[16] Muranaka S, Shinjo T, Bando Y and Takada T 1971 *J. Phys. Soc. Japan* **30** 890
[17] Gurewitz E and Atzmony U 1982 *Phys. Rev.* B **26** 6093
[18] Cruz J M R, Morais P C and Neto K S 1986 *Phys. Lett.* A **116** 45
[19] Grey I E and Ward J 1973 *J. Solid State Chem.* **7** 300
[20] Drofenik M, Golič L, Hanžel D, Kraševec V, Prodan A, Bakker M and Kolar D 1981 *J. Solid State Chem.* **40** 47
[21] Shiojiri M, Sekimoto S, Maeda T, Ikeda Y and Iwauchi K 1984 *Phys. Status Solidi* **84** 55
[22] Larson A C and von Dreele R B 1985–94 Los Alamos National Laboratory (LAUR 86-748, 1994)
[23] Bancroft G M *Mössbauer Spectroscopy: an Introduction for Inorganic Chemists and Geochemists* pp 157, 190–1
[24] Shannon R D and Prewitt C T 1969 *Acta Crystallogr.* B **25** 925